JOURNAL OF ADVANCED DIELECTRICS
Vol. 9, No. 6 (2019) 1950045 (8 pages)

DOI: 10.1142/S2010135X19500450

World Scientific
www.worldscientific.com

# Influence of transition metal ions on multiferroic properties of lead-free NBT–BT ceramics

S. Shanmuga Sundari*,†,‡ and R. Dhanasekaran*
*Crystal Growth Centre
Anna University, Chennai 600025
Tamil Nadu, India
†PSGR Krishnammal College for Women
Peelamedu, Coimbatore 641004
Tamil Nadu, India
‡shanmugi.s@gmail.com

Received 3 October 2019; Revised 25 November 2019; Accepted 17 December 2019; Published 4 February 2020

Using the conventional solid-state reaction method, 0.5 wt.% of $MnO_2$-, NiO-, $Cr_2O_3$-, $Fe_2O_3$- and $Co_2O_3$-added $0.94Na_{0.5}Bi_{0.5}TiO_3$ (NBT)–$0.06BaTiO_3$ (BT) ceramics were prepared. The perovskite nature of the prepared ceramics was analyzed by powder XRD and the surface morphology was studied by means of SEM. The dielectric analysis was carried out from room temperature to 350°C at various frequencies and the diffusive transition at the dielectric maxima confirmed the relaxor nature of the ceramics. Creation of oxygen vacancies by the possible substitution of ferromagnetic impurities decreased the dielectric constant and piezoelectric constant ($d_{33}$). The co-existence of ferromagnetism and the ferroelectricity was observed in the Mn, Ni, Co and Cr-added NBT–BT ceramics. The magnetic force microscopy (MFM) analysis was carried out to study the ferromagnetic domains in the prepared ceramic.

*Keywords*: Ceramics; ferroelectricity; piezoelectricity; atomic force microscopy.



## 1. Introduction

Nowadays, a key fascinating field is the enhancement of computer bit storage greater than binary. Co-existence of ferromagnetism and ferroelectricity in a single-phase material will solve this issue.[1] Recently, researchers predicted that magnetic fields can induce an electric polarization for magnetic writing/electric reading and electric fields can control magnetizations for electric writing/magnetic reading.[2] The simultaneous existence of ferroelectricity and ferromagnetism is termed as "multiferroicity". Materials with two or all the three ferroic properties such as ferroelectricity, ferromagnetism and ferroelasticity are termed as multiferroics.[3] The ferroelectricity requires fully-filled $d$ or $f$ orbitals to induce surface charge; on the contrary, the ferromagnetism requires partially-filled and empty $d$ or $f$ orbitals for the spin interactions.[4] A large number of multiferroic materials are investigated and most of them are perovskitic in nature. Interest on these types of materials got increased due to their great potential application and the physics attached to them. Multiferroics are found to be used in the fields of nonvolatile memory (MRAM, DRAM and Fe-RAM), device storage, sensor and actuator applications.[1,5]

Generation of ferromagnetism in nonmagnetic perovskite materials draws continuous attention. Suitable modification in $A$- and $B$-sites of the $ABO_3$ perovskite improves the ferroelectric and dielectric properties. In addition, these modifications may lead to the magnetic effect with proper dopants. By *ab initio* calculation, Nakayama Katayama-Yoshida reported that $BaTiO_3$ doped with Fe, Co, Ni and Mn is a promising material to achieve ferromagnetism.[6] Room-temperature ferromagnetism was achieved in Co-doped $BaSrTiO_3$ thin films.[4] Ferromagnetic behavior of the Fe-doped lead niobate–lead titanate[7] and the thickness dependence of ferromagnetism in Co-doped $BaTiO_3$ (Ref. 8) and Mn-doped $PbTiO_3$ (Ref. 9) were studied in detail by many researchers. The Fe and Co ion implantations on $BaTiO_3$ single crystals show ferromagnetic behavior[10] which gives new insight for multiferroics. The ferroelectric behavior of Fe-doped sodium bismuth titanate (NBT) was studied by Davies *et al.*[11] To the best of our knowledge there is no report on the influence of Cr, Co, Ni, Mn and Fe on sodium bismuth titanate–barium titanate (NBT–BT) ceramics in view of ferromagnetism.

NBT–BT is a well-known lead-free relaxor material. The $(1-x)Na_{0.5}Bi_{0.5}TiO_3$–$xBaTiO_3$ ($0.06 \le x \le 0.07$) in its morphotropic phase boundary (MPB) has the best relaxor property when compared to all other lead-free relaxors like KBT, KNN and their solid solution.[12,13] NBT–BT is an $ABO_3$ perovskite-type relaxor with the $A$-site being shared by the $Na^+$, $Bi^{3+}$ and $Ba^{2+}$ ions and the $B$-site being occupied by the $Ti^{4+}$ ions. In this work we focused on the effect of

ferromagnetic additives like Cr, Co, Ni, Mn and Fe in the NBT–BT ceramics on its MPB. The dielectric, ferroelectric and ferromagnetic behaviors of prepared ceramics were discussed in detail.

## 2. Experimental Methods

Conventional solid-state reaction method was used to prepare all the ceramics. High-purity (99.9%) $Na_2CO_3$, $BaCO_3$, $Bi_2O_3$, $TiO_2$, NiO, $Cr_2O_3$, $Co_2O_3$, $Fe_2O_3$ and $MnO_2$ were used as initial precursors. The oxides and carbonates were weighed according to the composition of 0.94 $(Na_{0.5}Bi_{0.5}TiO_3)$–$0.06(BaTiO_3)$ + 0.5 wt.% of $y(y = \text{NiO}, Cr_2O_3, Co_2O_3, Fe_2O_3$ and $MnO_2)$. The carbonates and oxides were mixed homogeneously in ethanol medium and calcined at 850°C for 4 h. The calcined powders were reground and mixed with binder (polyvinyl alcohol). After drying, pellets of the size 19-mm diameter and 1-mm thickness were made by applying a pressure of 300 MPa. The prepared discs were sintered at 1200°C for 4 h. The obtained ceramics were finely ground and subjected to powder X-ray diffraction (XRD) in the range of 10–80° of $2\theta$ with a step angle of 0.02° and a step time of 1 s using PANalytical diffractometer (Cu-$K_\alpha$ radiation) to confirm phase formation and crystalline nature. Surface morphology of the gold-coated sintered samples was studied by scanning electron microscopy (SEM; Carl Zeiss MA15/EVO18). The variations of dielectric constant with temperature at different frequencies were studied from room temperature to 350°C using Agilent E4980A impedance analyzer. Ceramics were poled by applying a field of 20–25 kV/cm at room temperature for 20 min. The piezoelectric co-efficient $d_{33}$ (pC/N) was measured using piezometer (PM300, Piezotest). The *P–E* hysteresis loop was recorded by the *P–E* loop tracer at room temperature. The *M–H* loop was recorded by the Lake Shore VSM 7410. The magnetic domain analysis was carried out by Park XE-100 model atomic force microscopy (AFM).

## 3. Results and Discussion

The structure of prepared ceramics was analyzed by means of powder XRD and the results are shown in Fig. 1(a). It shows that all the prepared ceramics are having a perovskite structure with *R*3*c* space group. The absence of secondary peaks in the XRD pattern shows that the magnetic additives were diffused into NBT–BT lattice forming a complete solid solution.

The addition of magnetic impurities like Mn, Ni, Cr and Co shifts the XRD peaks toward the higher angle side whereas Fe addition shifts the peaks toward the lower angle side. For better understanding, the (110) peak shifting is shown in Fig. 1(b). The ionic radius of $Ti^{4+}$ (0.74 Å) is large when compared to $Mn^{2+}$(0.67 Å), $Ni^{2+}$ (0.70 Å), $Cr^{3+}$ (0.615 Å) and $Co^{3+}$ (0.65 Å). The replacement of $Mn^{2+}$, $Ni^{2+}$, $Cr^{3+}$, $Fe^{3+}$ and $Co^{2+}$ ions in the $Ti^{4+}$-site of NBT–BT results in lattice contraction and this leads to the shifting of XRD peaks toward the higher angle side except in Fe–NBT–BT. The XRD peaks of Fe–NBT–BT shift toward the lower angle side and the same nature is obtained for the Fe-doped NBT and Fe-doped BT.[11]

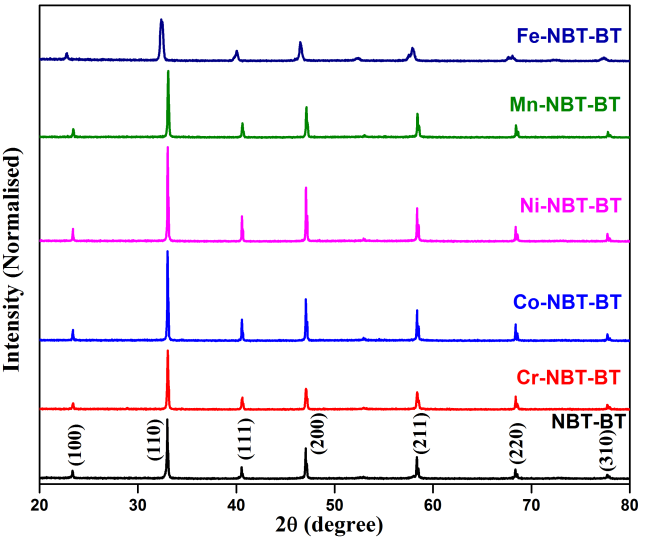


(a)

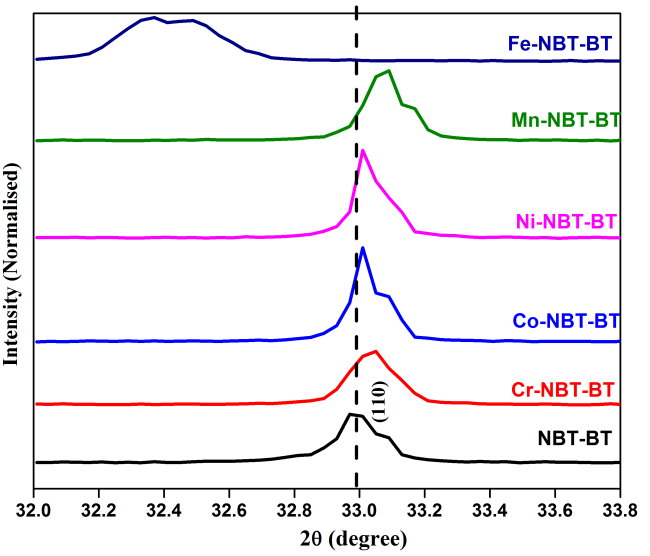


(b)

Fig. 1. (a) XRD patterns of synthesized ceramics. (b) Enlarged view of the (110) plane.

Besides the influence on the ferroelectric properties, added impurities alter the sinterability of the ceramic. Figure 2 shows the surface morphologies of prepared ceramics. All the prepared ceramics were dense and pore-free. The NBT–BT ceramics comprise cubic-like structure. For Co-, Mn- and Ni-added NBT–BT ceramics, the grains are like pebbles. In these, the edges of the grains are not sharp,

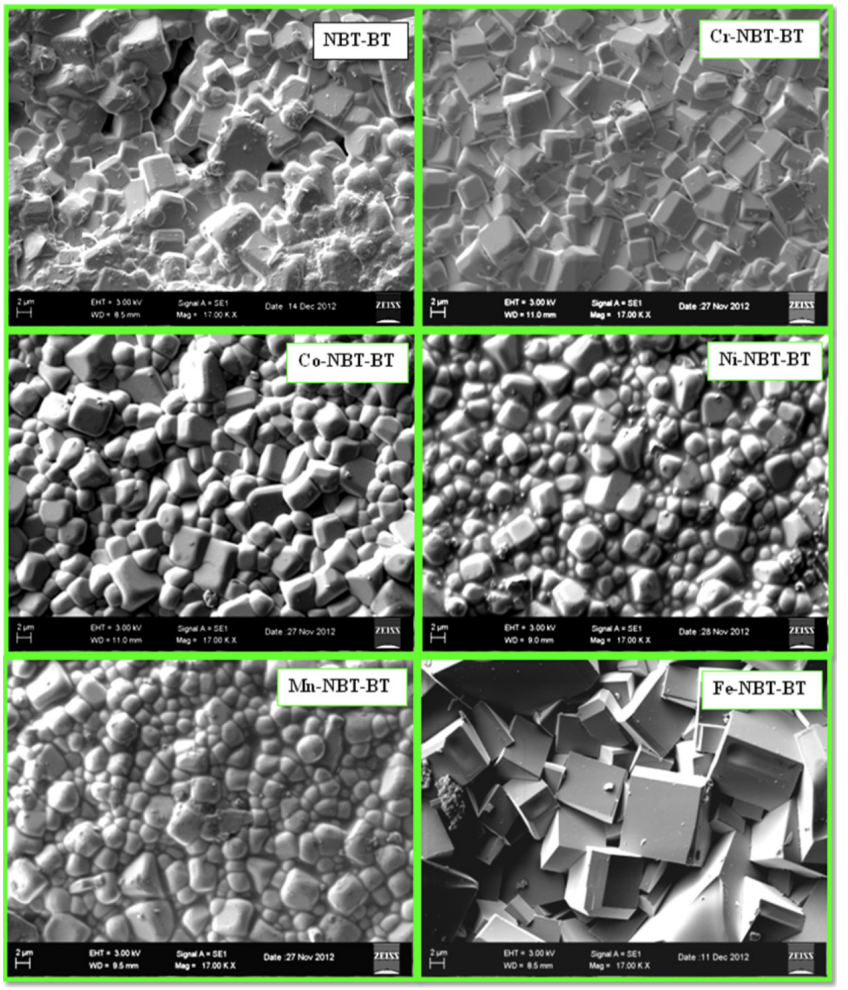


Fig. 2. SEM micrographs of NBT–BT, Cr–NBT–BT, Co–NBT–BT, Ni–NBT–BT, Mn–NBT–BT and Fe–NBT–BT.

which confirms the melting-like nature of the grains. This shows that the sintering temperature is high for these ceramics and the grain boundary contributions are increasing. For the addition of Fe and Cr rectangular grains were formed. The minimum and maximum sizes of the grains were observed in Mn–NBT–BT and Fe–NBT–BT, respectively. In addition, all the additives act like an acceptor dopant to the $Ti^{4+}$-site and oxygen vacancies are created to maintain the charge neutrality. These oxides precipitated at the grain boundary and controlled the grain growth.[14]

The dielectric analysis was carried out from room temperature (300 K) to 645 K at various frequencies and the results are shown in Fig. 3. The diffuse phase transition was observed in all the dielectric graphs. The dielectric maxima ($\varepsilon_m$) decreases as the measuring frequency increases and it shifts toward the higher temperature side. This is the main characteristic of the relaxor ferroelectric materials and arises due to the disordered lattice structure. The presence of nano-sized polar regions which originate from the cation displacements in the oxygen octahedral is the main cause for relaxor nature in $ABO_3$ perovskites.[15]

In all the dielectric graphs two dielectric anomalies one is at $T_d$ (temperature corresponding to the transition from ferroelectric to anti-ferroelectric) and another one is at $T_m$ (temperature corresponding to the transition from anti-ferroelectric to paraelectric and the temperature where dielectric constant reaches its maximum, $\varepsilon_m$), were observed except in Fe–NBT–BT. In Fe–NBT–BT the dielectric anomalies were observed only after 1 MHz. The multivalance nature of Fe creates electrical leakage problem and increases the conductivity of the sample. A similar scenario was observed by Cheng *et al.*[16] The values of $T_d$, $T_m$ and $\varepsilon_m$ (maximum dielectric constant) corresponding to 1-kHz measuring frequency are tabulated in Table 1 for all the samples.

The reduction of dielectric constant after the addition Mn, Ni and Cr is due to the grain size effect. The addition of Co increases the grain growth and hence the dielectric constant increases. Similarly for Fe addition, a maximum grain size was observed and so it exhibits the highest dielectric constant compared to all the additives. The value of $T_d$ decreases after the incorporation of Cr, Co, Mn and Ni in NBT–BT whereas the value of $T_m$ increases. The decrease in $T_d$ is attributed to the

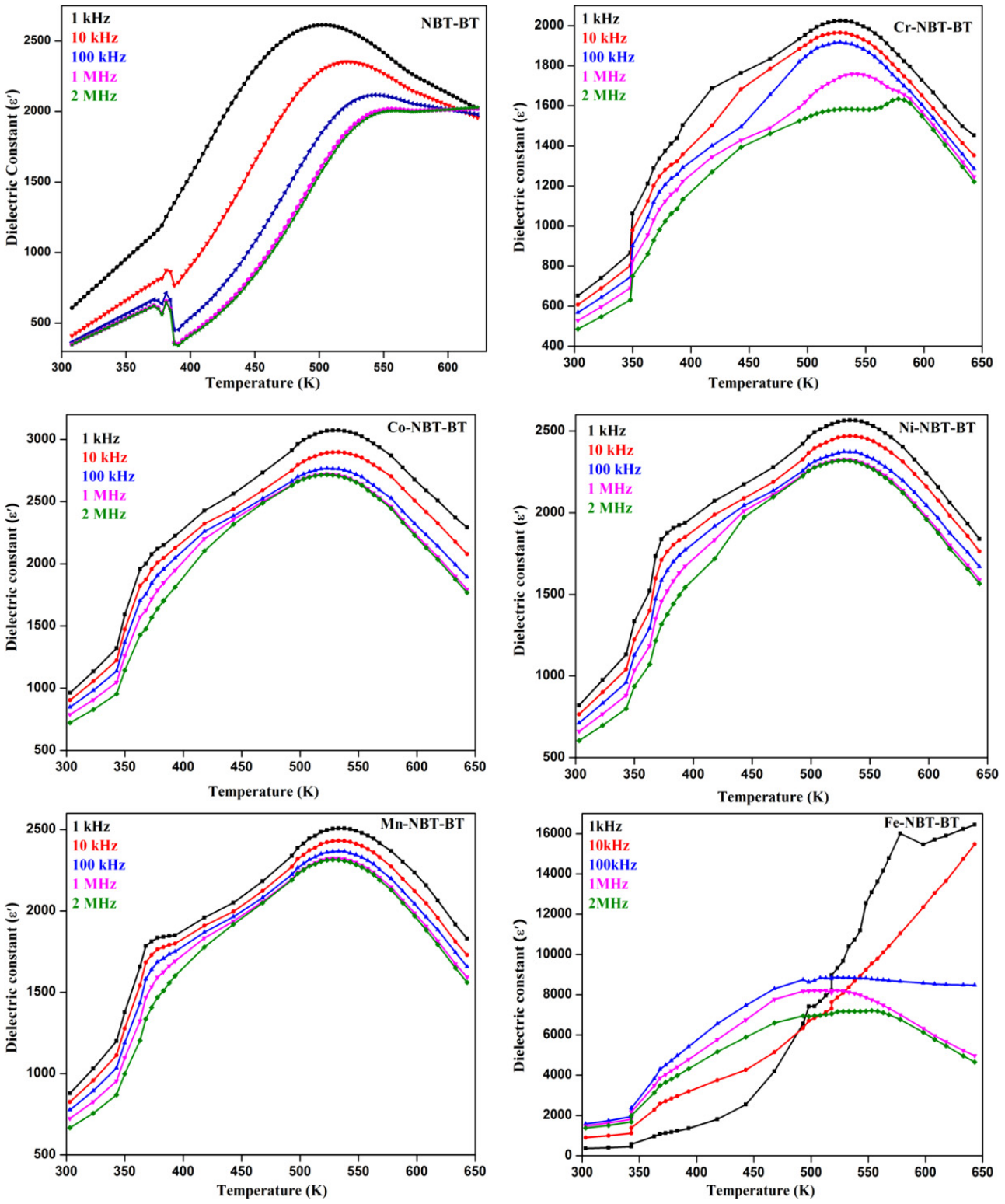


Fig. 3. Variations of dielectric constant as a function of temperature at various frequencies for all the synthesized ceramics.

decrease in grain size. The experimental data of the dielectric constant are fitted to the modified Curie–Weiss law[15] to analyze the diffusivity of the relaxation for all the samples. The calculated diffusivity parameter is listed in Table 1. Figure 4 shows the fitting of modified Curie–Weiss law for Cr–NBT–BT at 1 kHz. The diffusivity of the transition is increased for Ni and Mn additions. For the Co, Cr and Fe additions, $\gamma$ (diffusivity parameter) decreases. It has been suggested that the

Table 1. Values obtained from dielectric characteristics of synthesized ceramics.

| Sample | $T_d$ (K) | $T_m$ (K) | $\varepsilon_m$ | Γ |
|---|---|---|---|---|
| NBT–BT | 378 | 504 | 2680 | 1.79 |
| Cr–NBT–BT | 352 | 526 | 2023 | 1.70 |
| Co–NBT–BT | 372 | 530 | 3071 | 1.76 |
| Ni–NBT–BT | 373 | 536 | 2523 | 1.89 |
| Mn–NBT–BT | 357 | 534 | 2411 | 1.80 |
| Fe–NBT–BT (1 MHz) | — | 518 | 8212 | 1.31 |

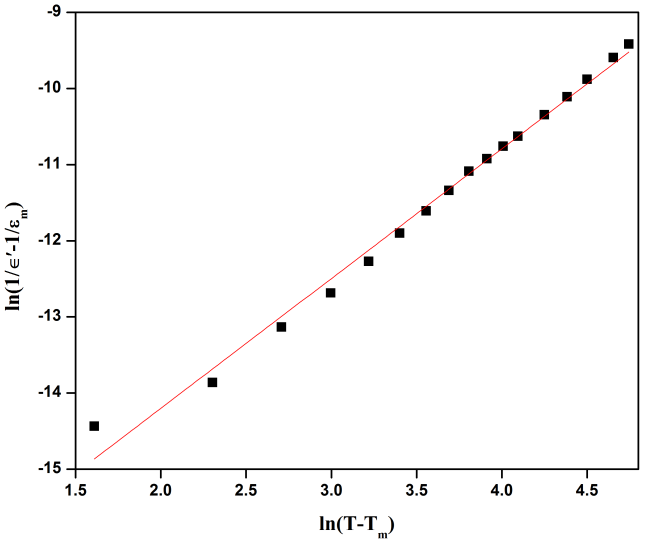


Fig. 4. Fitting of modified Curie–Weiss law for Cr–NBT–BT at 1 kHz.

relaxor behavior results from the *A*-site and *B*-site cation disorderings in $ABO_3$ perovskite structure. This reveals that the addition of Mn and Ni in NBT–BT strengthens the cation disordering and the compositional disorder.[17]

The electrode samples were poled at 2–2.5 kV/cm for 20 min and *P–E* hysteresis and piezoelectric coefficient ($d_{33}$) were measured at 1-kHz applied frequency. The measured $d_{33}$ values were 209, 119, 120, 139, 135 and 105 pC/N for NBT–BT, Cr–NBT–BT, Co–NBT–BT, Ni–NBT–BT, Mn–NBT–BT and Fe–NBT–BT ceramics, respectively. The $d_{33}$ was found to decrease after the addition of magnetic impurities. The added magnetic impurities replaced the Ti-site in $ABO_3$. The replacement in the *B*-site cation has a detrimental effect on the piezoelectric properties.[18,19] As discussed already, the oxygen vacancies restrict the grain growth and it leads to decrease in the interaction between the neighboring dipoles which is the main cause for the ferroelectric properties and it encourages domain wall pinning.

The *P–E* hysteresis loops are shown in Fig. 5. A well-saturated *P–E* loop was observed for Co–NBT–BT. The coercive field ($E_c$), remnant polarization ($P_r$) and the

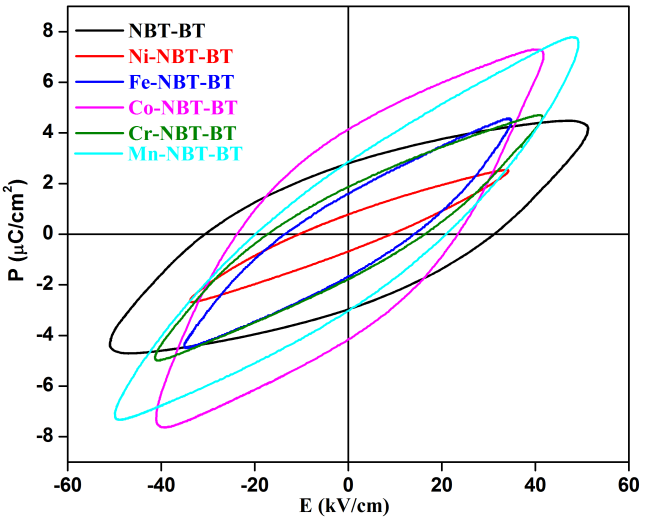


Fig. 5. *P–E* hysteresis loops for the synthesized ceramics.

Table 2. Ferroelectric and ferromagnetic properties of synthesized ceramics.

| | Ferroelectric hysteresis loop | | | Ferromagnetic hysteresis loop | | |
|---|---|---|---|---|---|---|
| Sample | $P_s$ (μC/cm²) | $P_r$ (μC/cm²) | $E_c$ (kV/cm) | $M_s$ (memu/g) | $M_r$ (memu/g) | $H_c$ (G) |
| NBT–BT | 4.39 | 2.77 | 31.2 | — | — | — |
| Cr–NBT–BT | 4.66 | 1.83 | 16.64 | 8.89 | 0.912 | 149.64 |
| Co–NBT–BT | 7.35 | 4.14 | 23.78 | 13.657 | 0.586 | 83.69 |
| Ni–NBT–BT | 2.58 | 0.77 | 9.49 | 9.25 | 0.892 | 123.89 |
| Mn–NBT–BT | 7.74 | 2.89 | 21.17 | 14.43 | 3.372 | 272.72 |
| Fe–NBT–BT | 4.57 | 1.60 | 14.13 | — | — | — |

saturation polarization ($P_s$) are listed in Table 2. The saturation polarization originates from the displacement of *B*-site cation in $ABO_3$ perovskite. Except for Ni–NBT–BT, the $P_s$ value increases for all other samples. The coercivity decreases

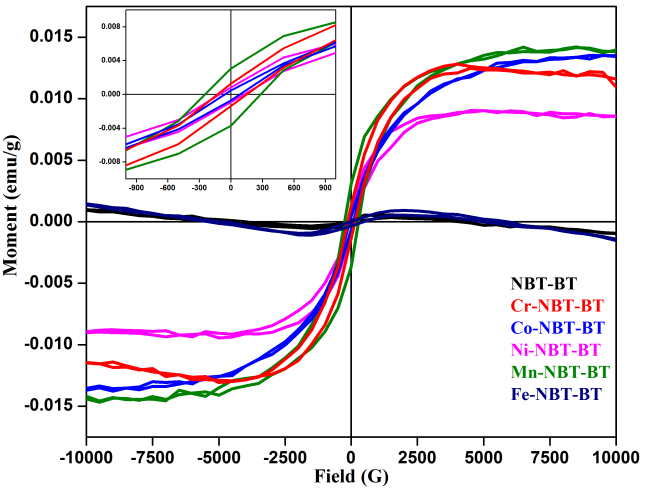


Fig. 6. *M–H* loops of synthesized ceramics at room temperature.

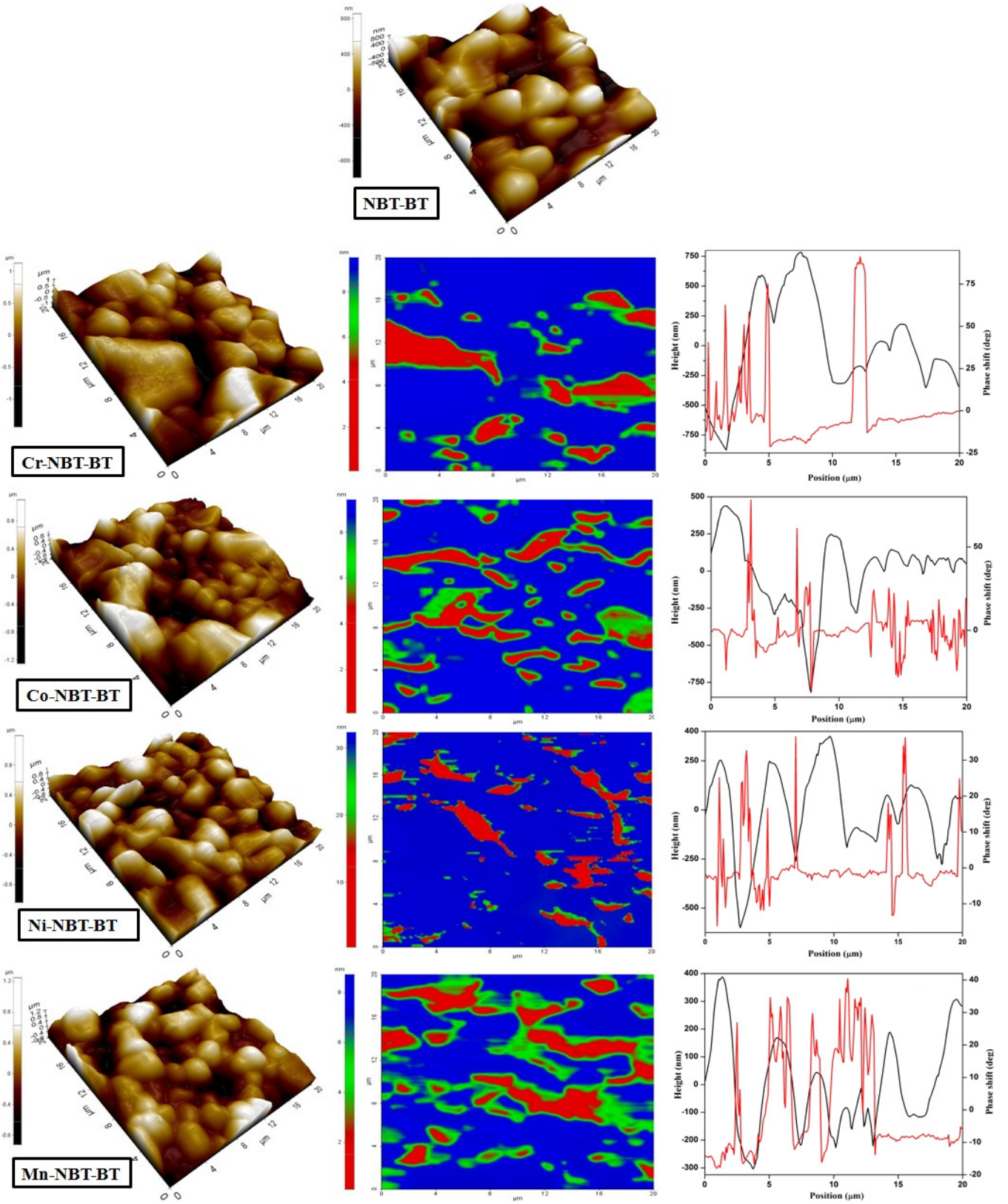


Fig. 7. Topographies, MFM phases and the line profiles.

considerably after the addition of magnetic impurities which enables them to be poled at high field also.

To study the magnetic properties, *M–H* curves for the prepared ceramics were recorded at the room temperature (see Fig. 6). The *M–H* curve analysis shows that the NBT–BT ceramics are diamagnetic in nature. After, the addition of ferromagnetic additives Co, Cr, Mn and Ni, the NBT–BT transforms into a ferromagnetic nature ceramic whereas the addition of Fe into NBT–BT retains the diamagnetic nature. The magnetic ion distance (Fe–Fe) may be large in the case of Fe–NBT–BT which cannot transfer spins to create the global magnetic property.[6] The magnetic ions $Co^{3+}$, $Cr^{3+}$, $Mn^{2+}$ and $Ni^{2+}$ are promising candidates for the observed magnetic property in NBT–BT. Because of the disordered distribution and lower concentration in NBT–BT, the nonlinear *M–H* loop was very slim. The slim hysteresis loop shows that the prepared ceramics are of soft magnetic type. The oxygen vacancies created by these impurities are for charge neutrality.[20] The super-exchange interaction between the magnetic ions in different occupational sites is facilitated by these oxygen vacancies. Kumar and Yadav discussed that the coupling between the mixed valance states of Mn ion provides a possibility to induce the double exchange effect of $Mn^{2+}$ and $Mn^{3+}$ or $Mn^{4+}$ and thus brings the magnetic property in Mn-doped $PbTiO_3$.[9]

The Mn has three ionic states namely $Mn^{2+}$, $Mn^{3+}$ and $Mn^{4+}$. Though the stable state of Mn is $Mn^{2+}$, sintering at high temperature oxidizes $Mn^{2+}$ to higher valance states like $Mn^{3+}$ or $Mn^{4+}$. The different valences of Mn determine the various properties of the materials. The $Mn^{3+}$ and $Mn^{4+}$ will not have any influence on the grain growth and they increase the dielectric constant thereby improving the ferroelectric properties. Contrarily, $Mn^{2+}$ will decrease the grain size when it replaces higher valance states (e.g., $Ti^{4+}$).[18] In this investigation, the entire above phenomenon has resulted and it confirms the existence of different ionic states of Mn in NBT–BT lattice. The multivalence nature of Mn in NBT was studied by ESR analysis.[21] The observed ferromagnetism in Mn–NBT–BT is due to the double exchange interactions between these $Mn^{2+}$ and $Mn^{4+}$ ions.

The stable states of Cr, Co and Ni in this case are $Cr^{3+}$, $Co^{3+}$ and $Ni^{2+}$, respectively. The other ionic states of these ions are possible only in $O_2$ or vacuum annealing. Hence during the super-exchange interactions between $Cr^{3+}$–$Cr^{3+}$, $Co^{3+}$–$Co^{3+}$ and $Ni^{2+}$–$Ni^{2+}$ ions, different occupational sites associated with oxygen vacancies are expected to produce the observed ferromagnetism in Cr–NBT–BT, Co–NBT–BT and Ni–NBT–BT. Fe-doped NBT ceramics showed diamagnetism till 0.6 mol.% of Fe and with further increase of Fe concentration, the ferromagnetism was observed. In our case also, Fe-added NBT–BT retained the diamagnetic behavior. This may be due to that the distance between Fe–Fe may be large in the case of Fe–NBT–BT which cannot transfer spins to create the global magnetic property.[6]

Magnetic domain analysis was carried out by means of magnetic force microscopy (MFM). MFM is a valuable tool to study the ferromagnetic domain structure and distribution of the sample with high lateral resolution. The MFM images correspond to the magnetic force emerging from the sample surface only. In this case, the cantilever was magnetized by an external magnet for 20 min to align the magnetic dipoles of the tip normal to the sample surface. The tip magnetization was negligible in all the measurements. The cantilever is in perpendicular orientation hence it is responsive only to the *x*-component of the spins which are in front and behind the cantilever.[22] In the MFM mode the cantilever will operate in noncontact and lift modes. To catch the magnetic signals the tip is elevated at the lift mode.

The tip to sample distance was maintained at 30 nm. Figure 7 shows the topographies, MFM phases and the line profiles corresponding to the topographies and the MFM phases. As the roughness of Fe–NBT–BT sample is in the order of 50 $\mu$m, AFM analysis cannot be carried out. From Fig. 7 there is no correlation between the topography and the MFM image. To stress that the line profiles of these two things are shown in the top-right corner of Fig. 7 for all the samples. Due to the magnetic interactions there are bright and dark regions in the MFM images and they correspond to the magnetic domains of opposite polarity. The presence of magnetic impurities is the soul responsible for the ferromagnetism observed in NBT–BT. The micrometer-sized domains indicate strong agglomeration of magnetic additives in NBT–BT ceramics. Among all the samples, maximum magnetic domain size was observed in Mn–NBT–BT and minimum was observed in Ni–NBT–BT.

## 4. Conclusion

The structural, dielectric, ferroelectric, piezoelectric and ferromagnetic properties were discussed in detail for the Cr-, Co-, Ni-, Mn- and Fe-added NBT–BT ceramics. The formation of complete solid solution after the addition of ferromagnetic additives in NBT–BT ceramics was observed in XRD analysis. From the diffuse phase transitions in the relaxor, the nature of synthesized ceramics was confirmed. The creation of oxygen vacancies by the *B*-site substitution decreases the dielectric constant and the piezoelectric properties. The room-temperature *M–H* hysteresis loop confirms the ferromagnetic nature. The exchange interaction between the ferromagnetic ions induces ferromagnetic nature in the diamagnetic NBT–BT. The ferromagnetic domain structures were analyzed by MFM. The coexistence of ferroelectric and ferromagnetic natures was found in Mn–NBT–BT, Ni–NBT–BT, Cr–NBT–BT and Co–NBT–BT ceramics. The order of the best multiferroics in this work is Mn–NBT–BT > Cr–NBT–BT > Ni–NBT–BT > Co–NBT–BT. A detailed ferromagnetic analysis will be the future scope of this work.

## References

[1]J. F. Scott, Applications of modern ferroelectrics, *Science* **315**, 954 (2007).
[2]N. Hur, S. Park, P. A. Sharma, J. S. Ahn, S. Guha and S. W. Cheong, Electric polarization reversal and memory in a multiferroic material induced by magnetic field, *Nature* **429**, 392 (2004).
[3]P. Lukashev, R. F. Sabirianov and K. Belashchenko, Theory of piezomagnetic effect in Mn-based antiperovskites, *Phys. Rev. B* **78**, 184414 (2008).
[4]Y.-H. Lin, S. Zhang, C. Deng, Y. Yang, X. Wang and C.-W. Nan, Magnetic behavior and thickness dependence in Co-doped $BaTiO_3$ thin films, *Appl. Phys. Lett.* **92**, 112501 (2008).
[5]J. W. Zhai, T. F. Hung and H. Chen, Relaxor and nonlinear behaviors of $SrTiO_3/BaTiO_3$ multilayers derived by a sol–gel process, *Appl. Phys. Lett.* **85**, 2026 (2004).
[6]H. Nakayama and H. Katayama-Yoshida, Theoretical prediction of magnetic properties of $Ba(Ti_{1-x}M_x)O_3$ ($M$ = Sc, V, Cr, Mn, Fe, Co, Ni, Cu), *Jpn. J. Appl. Phys.* **40**, L1355 (2001).
[7]Z. X. Cheng, X. L. Wang, G. Alvarez, S. X. Dou, S. J. Zhang and T. R. Shrout, Magnetic glassy behavior in ferroelectric relaxor type solid solutions: Magnetoelectric relaxor, *J. Appl. Phys.* **105**, 07D902 (2009).
[8]L. B. Luo, Y. G. Zhao, H. F. Tian, J. J. Yang and H. Y. Zhang, Room temperature ferromagnetism in the Co-doped $Ba_{0.5}Sr_{0.5}TiO_3$ thin film, *Appl. Phys. Lett.* **92**, 232507 (2008).
[9]M. Kumar and K. L. Yadav, Study of dielectric, magnetic, ferroelectric and magnetoelectric properties in the $PbMn_xTi_{1-x}O_3$, *J. Phys., Condens. Matter* **19**, 242202 (2007).
[10]N. I. Khalitov, R. I. Khaibulin, V. F. Valeev, E. N. Dulov, N. G. Ivoilov, L. R. Tagirov, S. Kazan, S. G. Sale and M. A. Mikailzade, Structural and magnetic studies of Co and Fe implanted $BaTiO_3$ crystals, *Nucl. Instrum. Methods Phys. Res. B* **272**, 104 (2012).
[11]M. Davies, E. Aksel and J. L. Jones, Enhanced high temperature piezoelectric coefficient and thermal stability of Fe and Mn substituted $Na_{0.5}Bi_{0.5}TiO_3$ ceramics, *J. Am. Ceram. Soc.* **94**, 1314 (2011).
[12]B. Babu, G. Madeswaran, M. He, D. F. Zang, X. L. Chen and R. Dhanasekaran, Inhomogeneity issues in the growth of $Na_{1/2}Bi_{1/2}TiO_3$-$BaTiO_3$ single crystals, *J. Cryst. Growth* **310**, 467 (2008).
[13]S. Shanmuga Sundari, B. Kumar and R. Dhanasekaran, Synthesis, dielectric and relaxation behavior of lead free NBT-BT ceramics, *Ceram. Int.* **39**, 555 (2013).
[14]S. B. Majumdar, B. Roy, R. S. Katiyar and S. B. Krupanidhi, Effect of neodymium (Nd) doping on the dielectric and ferroelectric characteristics of sol-gel derived lead zirconate titanate (53/47) thin films, *J. Appl. Phys.* **90**, 2975 (2001).
[15]G. A. Samara, The relaxational properties of compositionally disordered $ABO_3$ perovskites, *J. Phys., Condens. Matter* **15**, R367 (2003).
[16]Z. X. Cheng, A. H. Li, X. L. Wang, S. X. Dou, K. Ozawa and H. Kimura, Structure, ferroelectric properties, and magnetic properties of the La-doped bismuth ferrite, *J. Appl. Phys.* **103**, 07E507 (2008).
[17]G. A. Smolenskii, V. A. Isupov, A. I. Agranovskayaands and N. Popov, New ferroelectrics of complex composition, *Sov. Phys.-Solid State* **2**, 2651 (1961).
[18]J. Yang, X. J. Meng, M. R. Shen, L. Fang, J. L. Wang, T. Lin, J. L. Sun and J. H. Chu, Hopping conduction and low frequency dielectric relaxtion in 5 mol% Mn doped (Pb, Sr) $TiO_3$ films, *J. Appl. Phys.* **104**, 104113 (2008).
[19]B. J. Chu, D. R. Chen, G. R. Li and Q. R. Yin, Electrical properties of $Na_{1/2}Bi_{1/2}TiO_3$-$BaTiO_3$, *J. Eur. Ceram. Soc.* **22**, 2115 (2002).
[20]L. Gao, J. Zhai and X. Yao, The influence of Co doping on the dielectric, ferroelectric and ferromagnetic properties of $Ba_{0.70}Sr_{0.30}TiO_3$ thin films, *Appl. Surf. Sci.* **255**, 4521 (2009).
[21]W. Ge, H. Liu, X. Zhao, W. Zhong, X. Pan, T. He, D. H. Xu, X. Jiang and H. Luo, Growth, optical and electrical properties of pure and Mn-doped $Na_{0.5}Bi_{0.5}TiO_3$ lead-free piezoelectric crystals, *J. Alloys Compd.* **462**, 256 (2008).
[22]D. Rugar, R. Budakian, H. J. Mamin and B. M. Chul, Single spin detection by the magnetic resonance, *Nature* **430**, 329 (2004).